Development of Functionalized Materials Using Organometallic Compounds. IV.[1] Thermal Residual Stresses during the Fabrication of a Ni-Coated Continuous Carbon Fiber Aluminum Composites

Yozo MIKATA,† Tamotsu TAKAHASHI, Shuenn-Kung SU, and Yasuzo UCHIDA*
Department of Industrial Chemistry, Faculty of Engineering,
The University of Tokyo, Hongo, Bunkyo-Ku, Tokyo 113
†Department of Civil Engineering, Technological Institute, Northwestern University,
Evanston, IL 60201, U.S.A.
(Received December 18, 1986)

The thermal residual stresses during the fabrication of a Ni-coated carbon fiber composite are calculated by using two- and four-concentric-circular-cylinders models. The advantage of the CDL (chemical deposition in liquid phase) coating method at low temperature (200 °C), which is using organonickel compounds such as $Ni(cod)_2$ (cod=1,5-cyclooctadiene), over the conventional melted Ni-coating method (1453 °C) has been definitely confirmed from the crack prevention viewpoint.

There has been a growing interest in coated fiber composites such as electric composites or metal matrix composites. For such composites, the purpose of the coating on fiber is to develop a functionalized fiber or to serve as a chemical reaction barrier between the metal matrix and the fiber. We have recently reported that carbon materials were uniformly coated with metals such as Al,[2] Fe,[3] Co,[1] or Ni[1] at low temperature by the CDL method using organometallic compounds. Advantages of this CDL method have been investigated. This CDL method for an aluminum coating improved the wetting of carbon by aluminum metal and obviated the formation of aluminum carbide.[2] $Ni(cod)_2$ and $Co_2(CO)_8$, which do not have low boiling points, can be used by this CDL method for Co- and Ni-coating of carbon fibers, respectively, in sharp contrast to the CVD (chemical vapor deposition) method.

In order to evaluate the effect of the low coating temperature of the CDL method (ca. 200 °C) compared with the conventional nickel coating using melted nickel metal (1453 °C), we calculated the thermal residual stresses due to the mismatch of thermal expansion coefficients of its constituents. The thermal stresses in a coated short fiber composite[4] and in a coated continuous fiber composite[5] have been recently discussed by one of the authors. There have been a number of other works for a continuous fiber (not coated) composite,[6,7] and for a composite cylinder.[8,9] However, none of these works considered the thermal residual stresses of the coated continuous fiber composite during the fabrication process.

In this paper, specific emphasis will be given to the feasibility study of Ni-coated carbon fiber and its aluminum composite from the fabrication viewpoint. Two nickel coating methods were compared. One is the CDL method using organonickel compounds we recently reported.[1] The big advantage of this method is that the temperature at the time of coating is very low (about 200 °C) and to be controlled. The other is a conventional method in which nickel metal is heated up to its melting point (1453 °C) and coated on the carbon fiber. We will focus on the effect of the difference of these two temperatures on thermal residual stresses built up during the fabrication process.

Thermal Residual Stress. In the following analysis, we largely rely on the formulation presented in Ref. 4. For the sake of self containedness, however, we review some of the results reported before.[4]

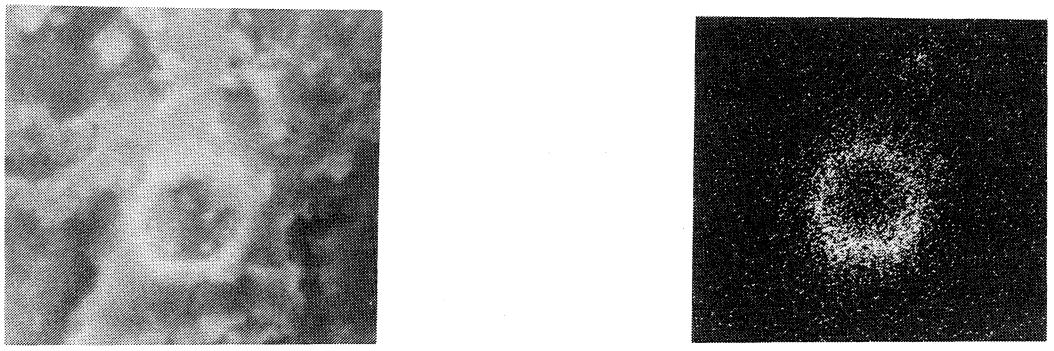

(A) SEM picture (B) Characteristic X-ray picture

Fig. 1. Cross section of Ni coated carbon fiber.

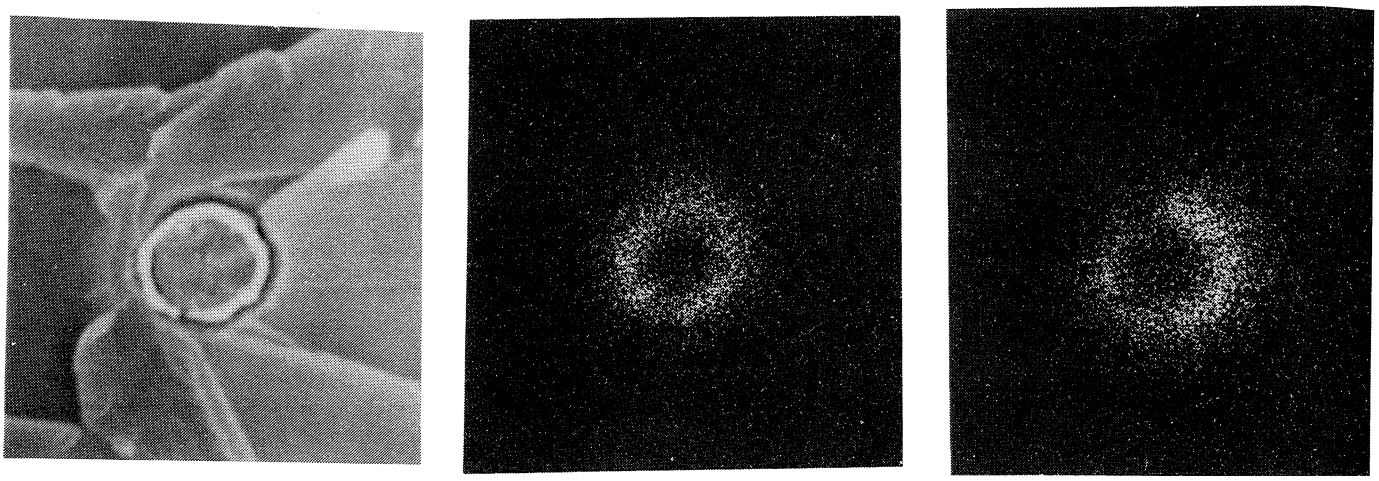

(A) SEM picture (B) Ni characteristic X-ray picture (C) Al characteristic X-ray picture

Fig. 2. Cross section of Al/Ni coated carbon fiber.

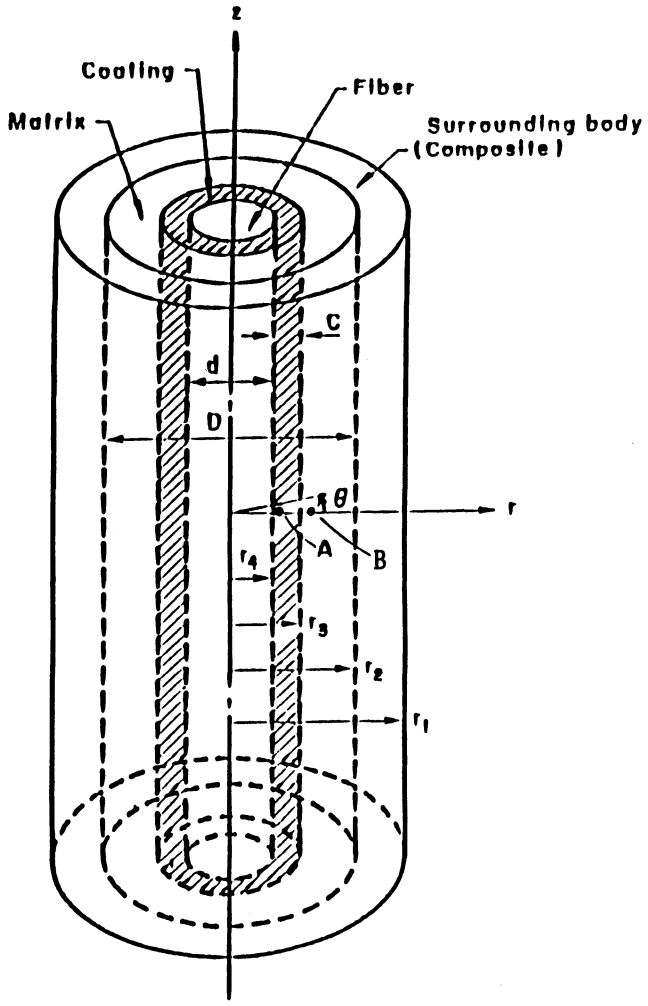

Fig. 3. Four phase model.

In order to evaluate the thermal residual stresses during the fabrication process, we need to consider two stages, stage-1: making the coated fiber, and stage-2: making the composite by combining the coated fiber and the matrix. At each stage, there are thermal residual stresses. The final thermal residual stresses are the sum of those stresses at stage 1 and 2.

Cross section of nickel-coated carbon fiber by the CDL method and that surrounded with aluminum are shown in Figs. 1 and 2. To simplify the calculations a coated continuous fiber composite is modeled as four concentric infinitely long circular cylinders (four phase model) as shown in Fig. 3. The surrounding body with the composite properties (outermost cylinder), matrix, coating and fiber (innermost cylinder) are denoted by domain 1, 2, 3, and 4, respectively, and their radii by r_1, r_2, r_3, and r_4, respectively. The diameters of fiber and matrix (including a coated fiber) are denoted by d and D, respectively, and the coating thickness by c. Since the surrounding body is infinite, r_1 will be made infinity at the end of the formulation.

To compute the thermal residual stresses at stage 1, we only need to consider two concentric circular cylinders, which consists of the fiber and the coating. Thermal residual stresses at stage 2 can be computed by using the four phase model described above.

Let us first obtain the thermal residual stresses at stage 1. The coating and the fiber are denoted as the domain 3 and 4, respectively, and the radii of the coating and the fiber as r_3 and r_4, respectively. Their surface of the coating is stress free at this stage. The constant temperature change is denoted as ΔT_1. The stress field is obtained in a similar manner as reported before[4] and given by

$$\sigma_{rr}^{(m),1} = C_{11}^{(m)}\left(A_m^1 - \frac{B_m^1}{r^2}\right) + C_{12}^{(m)}\left(A_m^1 + \frac{B_m^1}{r^2}\right) + C_{13}^{(m)}E^1 - \beta_1^{(m)}\Delta T_1$$
$$\sigma_{\theta\theta}^{(m),1} = C_{12}^{(m)}\left(A_m^1 - \frac{B_m^1}{r^2}\right) + C_{11}^{(m)}\left(A_m^1 + \frac{B_m^1}{r^2}\right) + C_{13}^{(m)}E^1 - \beta_1^{(m)}\Delta T_1 \quad (1)$$
$$\sigma_{zz}^{(m),1} = 2C_{13}^{(m)}A_m^1 + C_{33}^{(m)}E^1 - \beta_3^{(m)}\Delta T_1 \qquad m=3,4$$

with $B_4^1=0$, and where

$$\beta_1^{(m)} = (C_{11}^{(m)}+C_{12}^{(m)})\alpha_{mT} + C_{13}^{(m)}\alpha_{mL}$$
$$\beta_3^{(m)} = 2C_{13}^{(m)}\alpha_{mT} + C_{33}^{(m)}\alpha_{mL}, \qquad m=3,4 \quad (2)$$

$C_{ij}^{(m)}$ are elastic constants of the m-th material, and α_{mT} and α_{mL} are the thermal expansion coefficients of the m-th material along the transverse (r) and longitudinal (z) direction, respectively. The unknown coefficients A_3^1, A_4^1, B_3^1, E^1 are determined by solving the following simultaneous equations.

$$\begin{pmatrix} a_{11}^1 & a_{12}^1 & a_{13}^1 & 0 \\ a_{21}^1 & 0 & a_{23}^1 & a_{24}^1 \\ a_{31}^1 & a_{32}^1 & a_{33}^1 & a_{34}^1 \\ a_{41}^1 & a_{42}^1 & 0 & a_{44}^1 \end{pmatrix} \begin{pmatrix} A_3^1 \\ A_4^1 \\ B_3^1 \\ E^1 \end{pmatrix} = \begin{pmatrix} b_1^1 \\ b_2^1 \\ b_3^1 \\ b_4^1 \end{pmatrix} \quad (3)$$

where the explicit expressions of elements in the square matrix a_{ij}^1 and column vector b_i^1 are given in the Appendix A.

The thermal residual stresses in the stage 2 are obtained by using the four phase model.[4] Let us denote the constant temperature change as ΔT_2. Then we find the stress field as

$$\sigma_{rr}^{(n),2} = C_{11}^{(n)}\left(A_n^2 - \frac{B_n^2}{r^2}\right) + C_{12}^{(n)}\left(A_n^2 + \frac{B_n^2}{r^2}\right) + C_{13}^{(n)}E^2 - \beta_1^{(n)}\Delta T_2$$
$$\sigma_{\theta\theta}^{(n),2} = C_{12}^{(n)}\left(A_n^2 - \frac{B_n^2}{r^2}\right) + C_{11}^{(n)}\left(A_n^2 + \frac{B_n^2}{r^2}\right) + C_{13}^{(n)}E^2 - \beta_1^{(n)}\Delta T_2$$
$$\sigma_{zz}^{(n),2} = 2C_{13}^{(n)}A_n^2 + C_{33}^{(n)}E^2 - \beta_3^{(n)}\Delta T_2, \qquad n=1\text{—}4 \quad (4)$$

Table 1. Material Properties of Constituents of Coated Fiber Composite

Material	Matrix Al 6009	Fiber Graphite T300	Coating Ni
E_T (GPa)	69.0	22.0	207
E_L (GPa)	69.0	226	207
ν_{12}	0.33	0.42	0.31
ν_{13}	0.33	0.30	0.31
α_T (1/°C)	24.3×10^{-6}	27.0×10^{-6}	13.3×10^{-6}
α_L (1/°C)	24.3×10^{-6}	-1.50×10^{-6}	13.3×10^{-6}
σ_{ult} (GPa)	0.342	3.04	0.317
Mp (θ_m/°C)	650		1453

with $B_4^2=0$, and where

$$\beta_1^{(n)} = (C_{11}^{(n)}+C_{12}^{(n)})\alpha_{nT} + C_{13}^{(n)}\alpha_{nL}$$
$$\beta_3^{(n)} = 2C_{13}^{(n)}\alpha_{nT} + C_{33}^{(n)}\alpha_{nL}, \qquad n=1\text{—}4 \quad (5)$$

The simultaneous equations for the eight unknowns A_1^2, A_2^2, A_3^2, A_4^2, B_1^2, B_2^2, B_3^2, E^2 in (4) are given by

$$\begin{pmatrix} a_{11}^2 & a_{12}^2 & 0 & 0 & a_{15}^2 & a_{16}^2 & 0 & 0 \\ 0 & a_{22}^2 & a_{23}^2 & 0 & 0 & a_{26}^2 & a_{27}^2 & 0 \\ 0 & 0 & a_{33}^2 & a_{34}^2 & 0 & 0 & a_{37}^2 & 0 \\ a_{41}^2 & 0 & 0 & 0 & 0 & 0 & 0 & a_{48}^2 \\ a_{51}^2 & a_{52}^2 & 0 & 0 & a_{55}^2 & a_{56}^2 & 0 & a_{58}^2 \\ 0 & a_{62}^2 & a_{63}^2 & 0 & 0 & a_{66}^2 & a_{67}^2 & a_{68}^2 \\ 0 & 0 & a_{73}^2 & a_{74}^2 & 0 & 0 & a_{77}^2 & a_{78}^2 \\ a_{81}^2 & 0 & 0 & 0 & 0 & 0 & 0 & a_{88}^2 \end{pmatrix} \begin{pmatrix} A_1^2 \\ A_2^2 \\ A_3^2 \\ A_4^2 \\ B_1^2 \\ B_2^2 \\ B_3^2 \\ E^2 \end{pmatrix} = \begin{pmatrix} 0 \\ 0 \\ 0 \\ b_4^2 \\ b_5^2 \\ b_6^2 \\ b_7^2 \\ b_8^2 \end{pmatrix} \quad (6)$$

where the explicit expressions of elements in the square matrix a_{ij}^2 and column vector b_i^2 are given in the Appendix B.

The final thermal residual stresses are computed as

$$\sigma_{ij}^{(l),f} = \sigma_{ij}^{(l),1} + \sigma_{ij}^{(l),2}, \qquad l=1\text{—}4 \quad (7)$$

where we have the following specifications.

$$\sigma_{ij}^{(1),1} = \sigma_{ij}^{(3),1} = 0 \quad (8)$$

Results and Discussion

Two Ni-coating methods are compared from mechanics viewpoint. Let us call the conventional melted nickel coating method at 1453 °C as the method I, and the CDL method at 200 °C as the method II.

The representative material properties of the Ni-coated graphite fiber/aluminum 6009 are given in Table 1,[10] where the tensile strength is denoted by σ_{ult}. It should be noted in Table 1 that the engineering elastic constants, E_T, E_L, ν_{12}, ν_{13}, G_L, are given instead of C_{ij}. The elastic constants C_{ij} are related to the engineering elastic constants.[11] Material properties of the surrounding body (composite) are obtained by using a rule of mixture,

$$C_{ij}^{(1)} = V_m C_{ij}^{(2)} + V_c C_{ij}^{(3)} + V_f C_{ij}^{(4)}$$
$$\alpha_{1T} = V_m\alpha_{2T} + V_c\alpha_{3T} + V_f\alpha_{4T} \quad (9)$$
$$\alpha_{1L} = V_m\alpha_{2L} + V_c\alpha_{3L} + V_f\alpha_{4L}$$

where V_m, V_c, V_f are the volume fraction of the matrix, coating and fiber, respectively, and they are given by

$$V_m = 1 - \left(\frac{r_3}{r_2}\right)^2, \quad V_c = \left(\frac{r_3}{r_2}\right)^2 - \left(\frac{r_4}{r_2}\right)^2,$$
$$V_f = \left(\frac{r_4}{r_2}\right)^2 = \left(\frac{d}{D}\right)^2 \quad (10)$$

In the following figures, the stresses in the surrounding body are omitted, because they are either 0 ($=\sigma_z$) or so small (σ_r, σ_θ) to draw in those scales.

Thermal residual stresses of the coated fiber along the radial direction (r-axis) which are caused by the method I and II are shown in the Figs. 4 and 5, respectively. It is assumed in both cases that the coated fiber is cooled down to room temperature (25 °C) after completing the Ni-coating. The ratio of coating thickness to fiber diameter c/d is set to be 0.2143. It is easily seen from Fig. 4 that σ_z in the coating (Ni) is far greater than the tensile strength of Ni (317 MPa). Thus it is very likely that the Ni-coating will be completely cracked, if we use the method I. Whereas, in the Fig. 5, it is seen that the maximum tensile stress (σ_z) in the Ni-coating is less than its tensile strength.

The final thermal residual stresses of the composite caused by the method II are shown in the Fig. 6. The

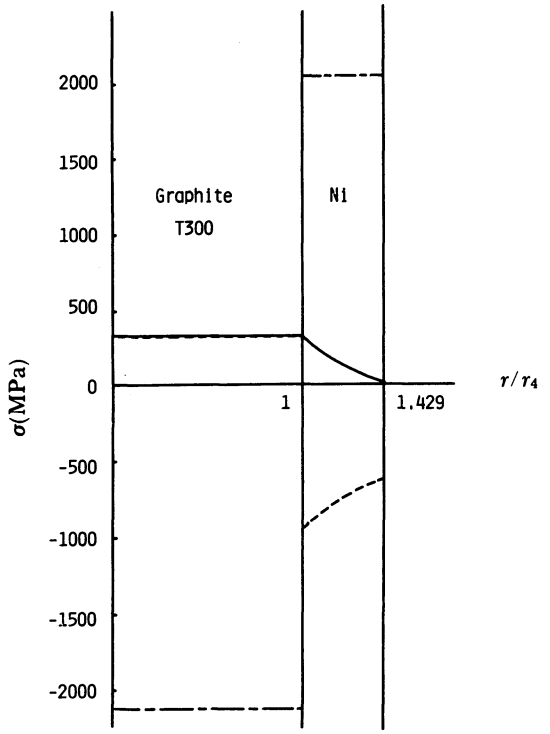

Fig. 4. Thermal residual stresses of the fiber caused by the method I (1453 °C—25 °C). $\Delta T=-1428$ °C, $c/d=15/70$. ——σ_r, ------σ_θ, —·—σ_z.

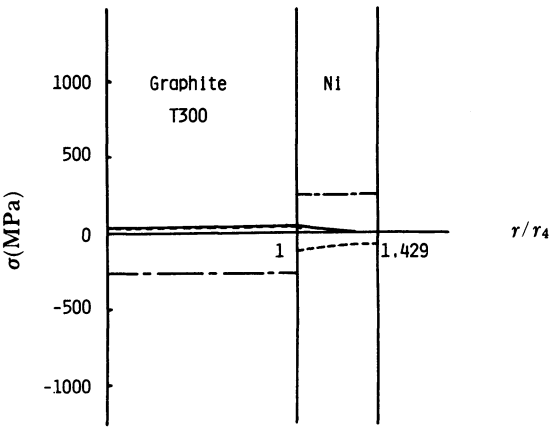

Fig. 5. Thermal residual stresses of the coated fiber caused by the method II. (200 °C—25 °C) $\Delta T=-175$ °C, $c/d=15/70$, ——σ_r, ------σ_θ, —·—σ_z.

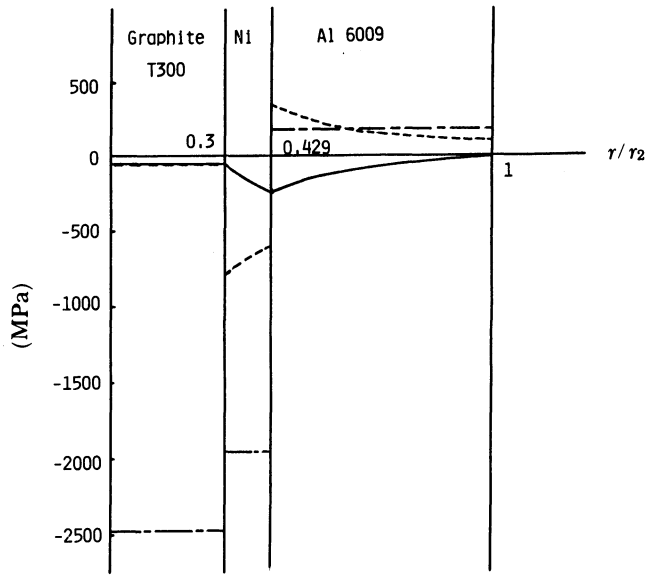

Fig. 6. Final thermal residual stresses of the composite by the method II. Coated fiber: 200 °C—(25 °C)—650 °C—25 °C, composite: 650 °C—25 °C. $V_f=0.09$, $c/d=15/70$, ——σ_r, ------σ_θ, —·—σ_z.

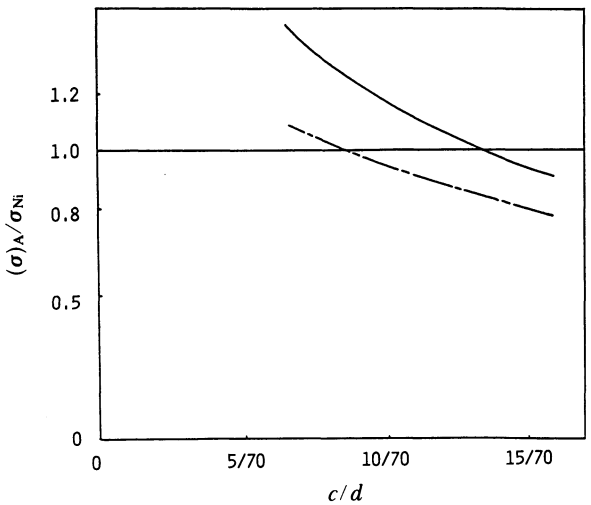

Fig. 7. Residual tensions of the coated fiber at a point A caused by the method II as a function of c/d. The stresses are normalized by the tensile strength of Ni. ——$(\sigma_\theta)_A/\sigma_{Ni}$, $\Delta T=450$ °C, 200 °C—(25 °C)—650 °C; —·—$(\sigma_z)_A/\sigma_{Ni}$, $\Delta T=-175$ °C, 200 °C—25 °C; $\sigma_{Ni}=317$ MPa.

volume fraction of the fiber V_f and the ratio of coating thickness to fiber diameter c/d set to be 0.09 and 0.2143, respectively. These values have been determined so as to make the maximum tensile stress occurring in each phase of the composite less than its tensile strength. It is observed in the Fig. 6 that the highest tensile residual stress (σ_θ) is formed at a point B (see Fig. 3). Even though this stress ($(\sigma_\theta)_B$=341.69 MPa) is almost reaching the tensile strength (342 MPa) of Al 6009, it is expected that the stress is somewhat relaxed by a possible plastic deformation of Al 6009, which our elastic calculation cannot predict. It is generally true that our elasticity assumption of the model gives rise to a higher stress value than expected in reality.

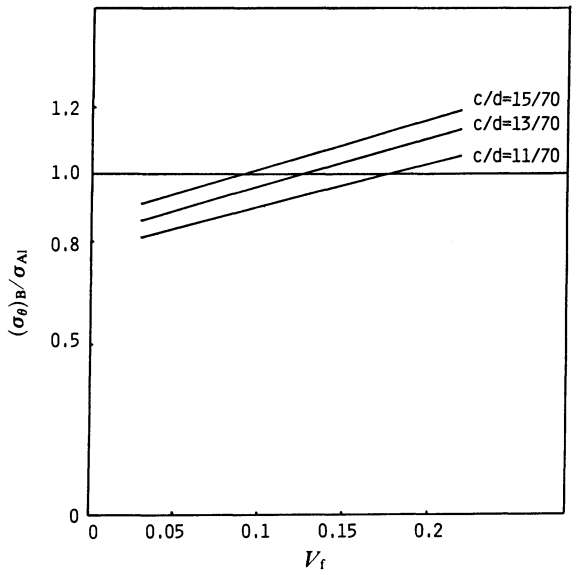

Fig. 8. Residual tension σ_θ of the composite at a point B caused by the method II as a function of V_f for various values of c/d. The stresses are normalized by the tensile strength of Al. ΔT=−625 °C, 650 °C—25 °C, σ_{Al}=342 MPa.

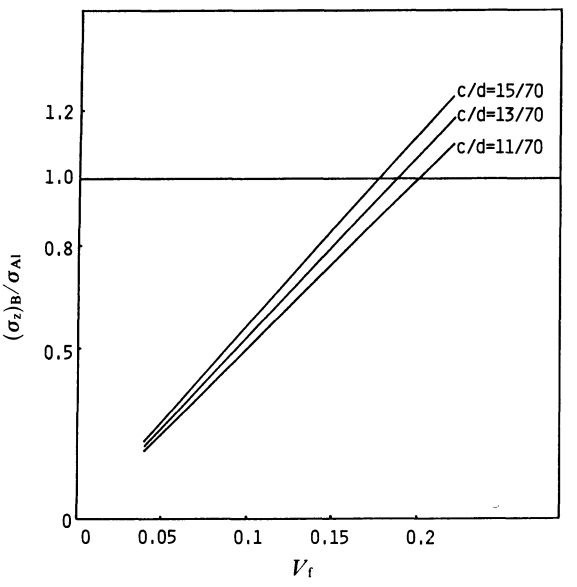

Fig. 9. Residual tension σ_z of the composite at a point B caused by the method II as a function of V_f for various values of c/d. The stresses are normalized by the tensile strength of Al. ΔT=−625 °C, 650 °C—25 °C, σ_{Al}=342 MPa.

A parametric study has been conducted by changing two parameters, i.e. V_f=0.04, 0.09, 0.16, and c/d= 11/70, 13/70, 15/70. Some of the highest tensile stresses occurring at each stage of the fabrication of the composite are drawn in the Figs. 7—9. In the Fig. 7, residual tensions of the coated fiber at a point A (see Fig. 3), caused by the method II are shown as a function of c/d. It is seen in this Figure that the residual tensions decrease as the ratio of coating thickness to fiber diameter c/d increases. In the Figs. 8 and 9, residual tensions σ_θ and σ_z of the composite at a point B caused by the method II are shown as a function of V_f for various values of c/d. It follows from Figs. 8 and 9 that the residual tensions increase as V_f and c/d increase.

Conclusion

(1) It was found that the melted Ni-coating method (method I) gives rise to a tremendous amount of tension (σ_z) in Ni phase, which presumably leads to cracking of Ni coating. Thus the method I is not desirable as a coating method of Ni on a carbon fiber.

(2) With suitable choices of geometrical parameters, it was found possible to make a Ni-coated graphite fiber/Al 6009 composite without cracking in any phase of the composite by the CDL method using organonickel compound (method II). It has been shown from this parametric study that, in general, the residual tension may be kept below the tensile strength of the material, if we design the composite so as to have sufficiently large c/d and sufficiently small V_f.

(3) Coupled with a possible applied stress field, however, the residual tension (σ_θ and σ_z) in Al phase may reach the tensile strength of Al rather easily. To reduce the residual tension, it would be desirable to lower the fabrication temperature of the composite by the CDL method using triisobutylaluminum for Al.[2)]

(4) It should be also noted that since our calculation is based on the elasticity assumption of the model, it tends to give rise to a higher residual tension. Thus we may be able to fabricate a flawless composite even with a slightly smaller ratio of coating thickness to fiber diameter c/d, and with a slightly larger volume fraction of the fiber V_f than prescribed by our calculation.

Appendix A

$$a^1_{11} = r_4,\quad a^1_{12} = -r_4,\quad a^1_{13} = \frac{1}{r_4}$$

$$a^1_{21} = -(C^{(3)}_{11}+C^{(3)}_{12}),\quad a^1_{23} = \frac{1}{r_3^2}(C^{(3)}_{11}-C^{(3)}_{12}),\quad a^1_{24} = -C^{(3)}_{13}$$

$$a^1_{31} = C^{(3)}_{11} + C^{(3)}_{12},\quad a^1_{32} = -(C^{(4)}_{11}+C^{(4)}_{12}),$$

$$a^1_{33} = -\frac{1}{r_4^2}(C^{(3)}_{11}-C^{(3)}_{12}),\quad a^1_{34} = C^{(3)}_{13} - C^{(4)}_{13}$$

$$a^1_{41} = 2C^{(3)}_{13}(r_3^2-r_4^2),\quad a^1_{42} = 2C^{(4)}_{13}r_4^2,\quad a^1_{44} = C^{(3)}_{33}(r_3^2-r_4^2) + C^{(4)}_{33}r_4^2$$

and

$$b^1_1 = 0,\quad b^1_3 = -\beta^{(3)}_1\Delta T_1,\quad b^1_3 = (\beta^{(3)}_1-\beta^{(4)}_1)\Delta T_1$$

$$b^1_4 = \beta^{(3)}_3(r_3^2-r_4^2)\Delta T_1 + \beta^{(4)}_3 r_4^2\Delta T_1$$

Appendix B

$$a^2_{11} = r_3,\quad a^2_{12} = -r_2,\quad a^2_{15} = \frac{1}{r_2},\quad a^2_{16} = -\frac{1}{r_2}$$

$$a^2_{22} = r_3,\quad a^2_{23} = -r_3,\quad a^2_{26} = \frac{1}{r_3},\quad a^2_{27} = -\frac{1}{r_3}$$

$$a^2_{33} = r_4,\quad a^2_{34} = -r_4,\quad a^2_{37} = \frac{1}{r_4},$$

$$a^2_{41} = -(C^{(1)}_{11}+C^{(1)}_{12}),\quad a^2_{48} = -C^{(1)}_{13},$$

$$a^2_{51} = C^{(1)}_{11} + C^{(1)}_{12},\quad a^2_{52} = -(C^{(2)}_{11}+C^{(2)}_{12})$$

$$a^2_{55} = -\frac{C^{(1)}_{11}-C^{(1)}_{12}}{r_2^2},\quad a^2_{56} = \frac{C^{(2)}_{11}-C^{(2)}_{12}}{r_2^2},\quad a^2_{58} = C^{(1)}_{13}-C^{(2)}_{13}$$

$$a^2_{62} = C^{(2)}_{11} + C^{(2)}_{12},\quad a^2_{65} = -(C^{(3)}_{11}+C^{(3)}_{12})$$

$$a^2_{66} = -\frac{C^{(2)}_{11}-C^{(2)}_{12}}{r_3^2},\quad a^2_{67} = \frac{C^{(3)}_{11}-C^{(3)}_{12}}{r_3^2},\quad a^2_{68} = C^{(2)}_{13} - C^{(3)}_{13}$$

$$a^2_{78} = C^{(3)}_{11} + C^{(3)}_{12},\quad a^2_{74} = -(C^{(4)}_{11}+C^{(4)}_{12})$$

$$a^2_{77} = -\frac{(C^{(3)}_{11}-C^{(3)}_{12})}{r_4^2},\quad a^2_{78} = C^{(3)}_{13} - C^{(4)}_{13}$$

$$a^2_{81} = 2C^{(1)}_{13},\quad a^2_{88} = C^{(1)}_{33}$$

and

$$b^2_4 = -\beta^{(1)}_1\Delta T_2,\quad b^2_5 = (\beta^{(1)}_1-\beta^{(2)}_1)\Delta T_2,\quad b^2_6 = (\beta^{(2)}_1-\beta^{(3)}_1)\Delta T_2$$

$$b^2_7 = (\beta^{(3)}_1-\beta^{(4)}_1)\Delta T_2,\quad b^2_8 = \beta^{(1)}_3\Delta T_2$$

References

1) Part 3. S.-K. Su, M. Akiba, T. Takahashi, M. Saburi, M. Hidai, and Y. Uchida, *Chem. Lett.*, **1987**, 337.

2) S.-K. Su, T. Takahashi, T. Kodama, M. Hidai, and Y. Uchida, *Nippon Kagaku Kaishi*, **1985**, 629.

3) S.-K. Su, T. Takahashi, T. Kodama, M. Hidai, and Y. Uchida, *Nippon Kagaku Kaishi*, **1987**, 877.

4) Y. Mikata and M. Taya, *J. Comp. Mater.*, **19**, 554 (1985).

5) Y. Mikata and M. Taya, *J. Appl. Mech.*, **53**, 681 (1986).

6) T. Ishikawa, K. Koyama, and S. Kobayashi, *J. Comp. Mater.*, **12**, 153 (1978).

7) M. Uemura, H. Iyama, and Y. Yamaguchi, *J. Thermal Stress*, **2**, 393 (1979).

8) D. Iesan, *J. Thermal Stress*, **3**, 495 (1980).

9) Y. Takeuchi, T. Furukawa, and Y. Tanigawa, "The effect of thermoelastic coupling for transient thermal stresses in a composite cylinder," ASME, WAM, DE-2 (1983).

10) "Metals Handbook," 9th ed, ed by T. Lyman, American Society for Metals, Vol. 2 (1979).

11) H. A. Elliot, *Proc. Camb. Phil. Soc.*, **44**, 522 (1948).